Cell Reports, Volume *35*

Supplemental information

Tau seeds are subject to aberrant modifications resulting in distinct signatures

Jui-Heng Tseng, Aditi Ajit, Zarin Tabassum, Niyati Patel, Xu Tian, Youjun Chen, Alex W. Prevatte, Karen Ling, Frank Rigo, Rick B. Meeker, Laura E. Herring, and Todd J. Cohen

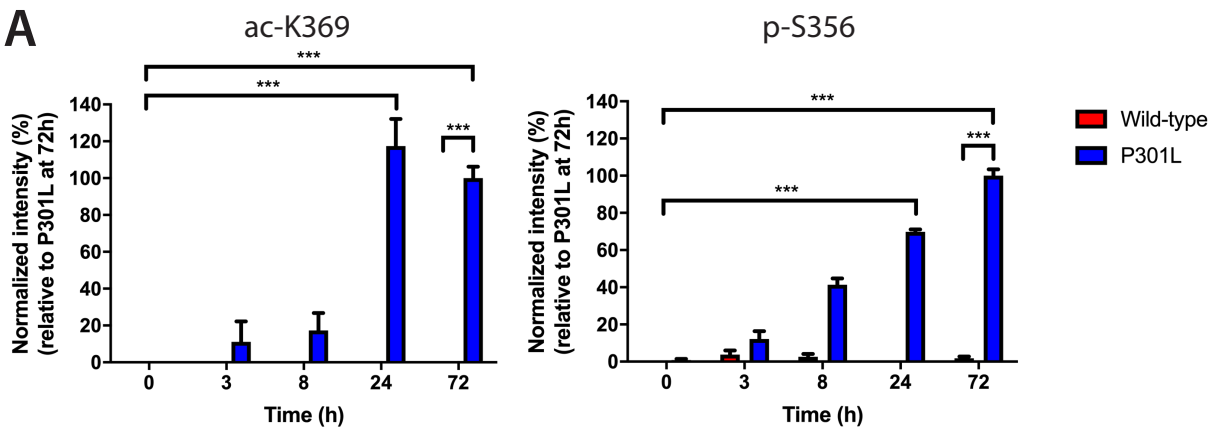

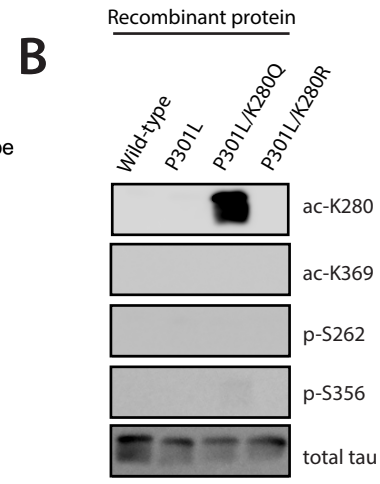

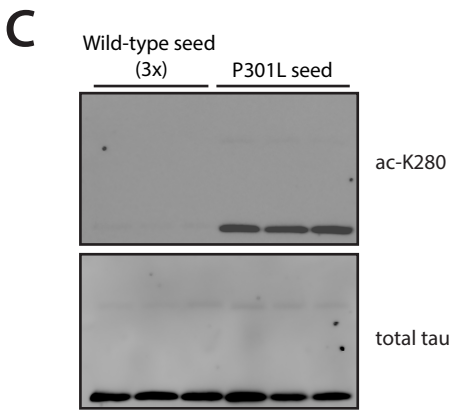

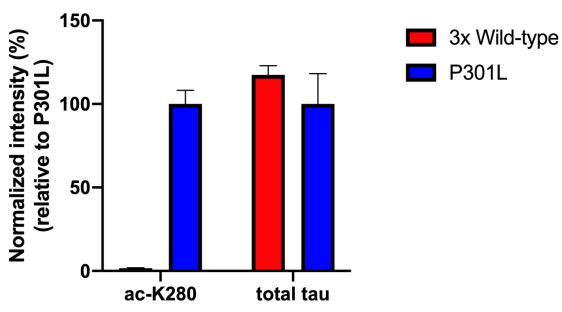

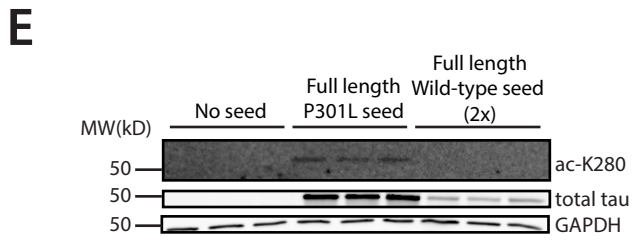

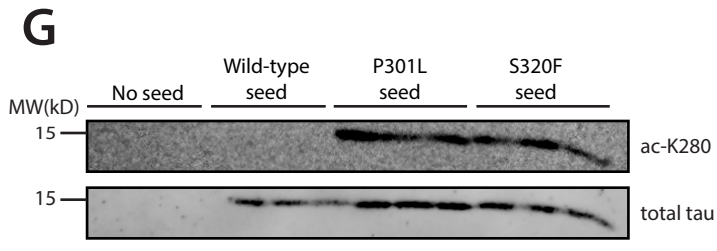

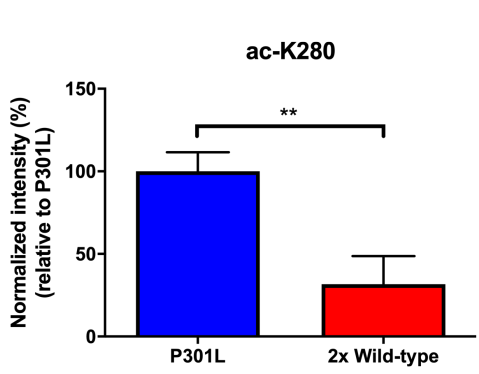

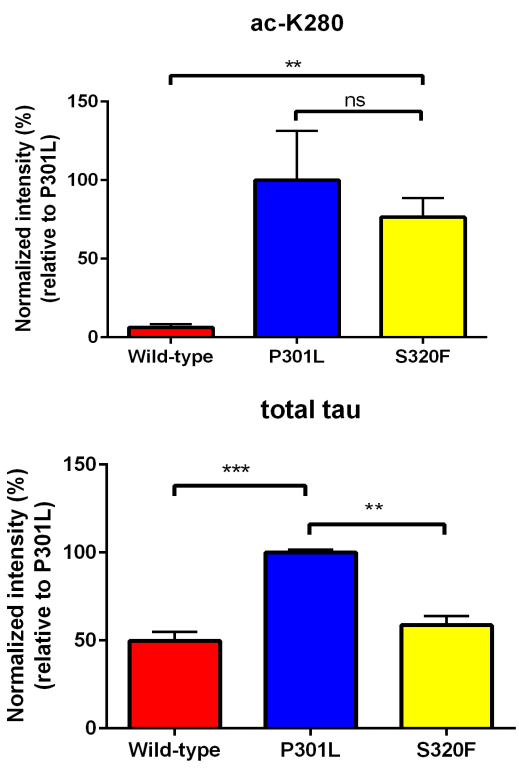

Figure S1. Internalized tau seeds show distinct post-translational modification (PTM) profiles, Related to Figure 1

(A) Primary cortical neurons were treated with wild-type or P301L tau seeds for 0-72 h. Quantification by densitometry shows that the levels of ac-K369 and p-S356 of P301L tau seed are significantly increased by 24 h. The extent of tau modifications was normalized to total tau seed level. Error bars indicate SEM; n = 3 biologically independent experiments. p value was determined by unpaired t test. *** $p < 0.001$.

(B) Recombinant wild-type, P301L, P301L/K280Q, and P301L/K280R tau monomers were immunoblotted with two acetylated (ac-K280, ac-K369), two phosphorylated (p-S262, p-S356), and total tau antibodies to analyze PTMs on recombinant purified tau proteins.

(C) Primary neurons were analyzed using 3-fold more lysate (3x) from neurons treated with wild-type vs. P301L tau seeds by immunoblotting with ac-K280 and total tau antibodies.

(D) Quantification of immunoblots in which 3x more wild-type lysates were compared to 1x P301L tau lysates. Error bars indicate SEM.

(E) Full-length (2N4R) wild-type or P301L tau seeds were added to primary neurons, and tau acetylation was analyzed by using ac-K280 antibody. Total tau and GAPDH served as loading controls.

(F) Quantification of ac-K280 immunoreactivity for full-length wild-type or P301L tau seeds. Error bars indicate SEM; n = 3 biologically independent experiments. p value was determined by unpaired t test. ** $p < 0.01$.

(G) Primary neurons were treated with wild-type, P301L, or S320F seeds (two different FTDP-17 disease variants) and analyzed by ac-K280 and total tau antibodies to evaluate tau seed acetylation.

(H) Quantification of wild-type, P301L, or S320F tau seeds with tau acetylation or total tau antibodies. Error bars indicate SEM; n = 3 biologically independent experiments. p value was determined by unpaired t test. n.s. $p > 0.05$, ** $p < 0.01$, *** $p < 0.001$.

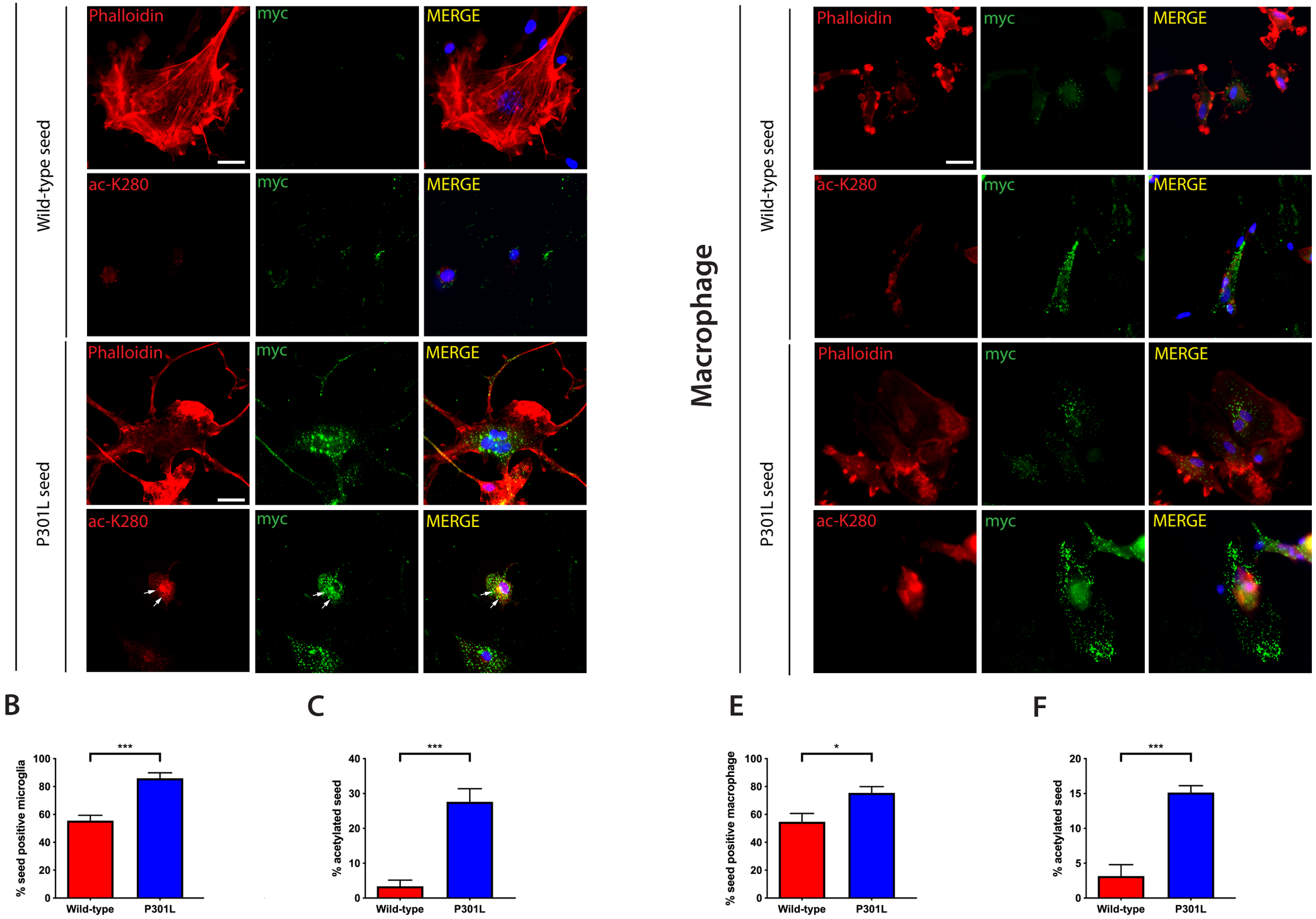

Figure S2. Disease-associated tau seeds are modified in a cell type-specific manner, Related to Figure 1

(A) Primary mouse microglia were treated with myc-tagged wild-type or P301L tau seeds for 2 days and analyzed by double labeling with the Alexa Fluor 594 Phalloidin or ac-K280 tau antibody (red) in combination with myc antibody (green). Arrows indicate acetylated seeds. Scale bar, 50 µm.

(B) Quantification of microglia containing tau seeds was determined as a ratio of the number of tau seed positive microglia to total microglia. Error bars indicate SEM; n = 4 biologically independent experiments. p value was determined by unpaired t test. *** $p < 0.001$.

(C) Percentage of acetylated seed was determined as a ratio of the number of ac-K280 positive tau seed to total tau seeds. Error bars indicate SEM; n = 4 biologically independent experiments. p value was determined by unpaired t test. *** $p < 0.001$.

(D) Primary human monocyte-derived macrophages (hMDMs) were treated with myc-tagged wild-type or P301L tau seeds for 2 days and analyzed by double labeling with the Alexa Fluor 594 Phalloidin or ac-K280 tau antibody (red) in combination with myc antibody (green). Arrows indicate acetylated seeds. Scale bar, 50 µm.

(E) Quantification of macrophage containing tau seeds was determined as a ratio of the number of tau seed positive macrophage to total macrophage. Error bars indicate SEM; n = 4 biologically independent experiments. p value was determined by unpaired t test. * $p < 0.05$.

(F) Percentage of acetylated seed was determined as a ratio of the number of ac-K280 positive tau seed to total tau seeds. Error bars indicate SEM; n = 4 biologically independent experiments. p value was determined by unpaired t test. *** $p < 0.001$.

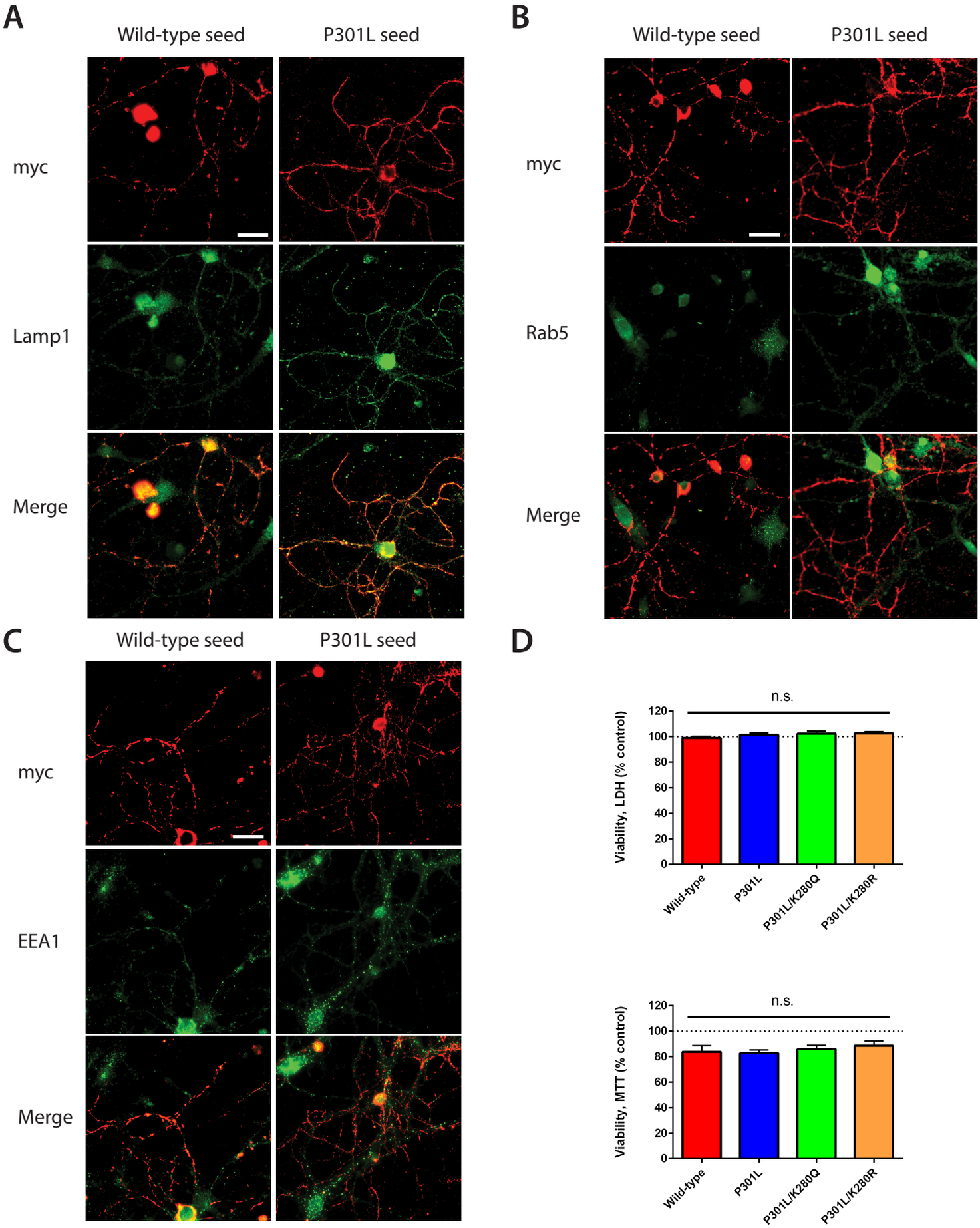

Figure S3. Tau seeds are internalized into intracellular vesicles but do not cause overt neuronal cell death or metabolic dysfunction, Related to Figure 2

(A-C) Primary neurons were treated with myc-tagged wild-type or P301L tau seeds and analyzed by double-labeling with a myc antibody (red) to mark myc-tagged tau seeds in combination with **(A)** Lamp1, **(B)** Rab5, or **(C)** EEA1 antibodies (green). Scale bar, 50 µm.

(D) LDH and MTT cell viability assays were performed on primary neurons treated with wild-type, P301L, P301L/K280Q, or P301L/K280R tau seeds. Error bars indicate SEM; n = 4 biologically independent experiments. p value was determined by one-way ANOVA. n.s. $p > 0.05$.

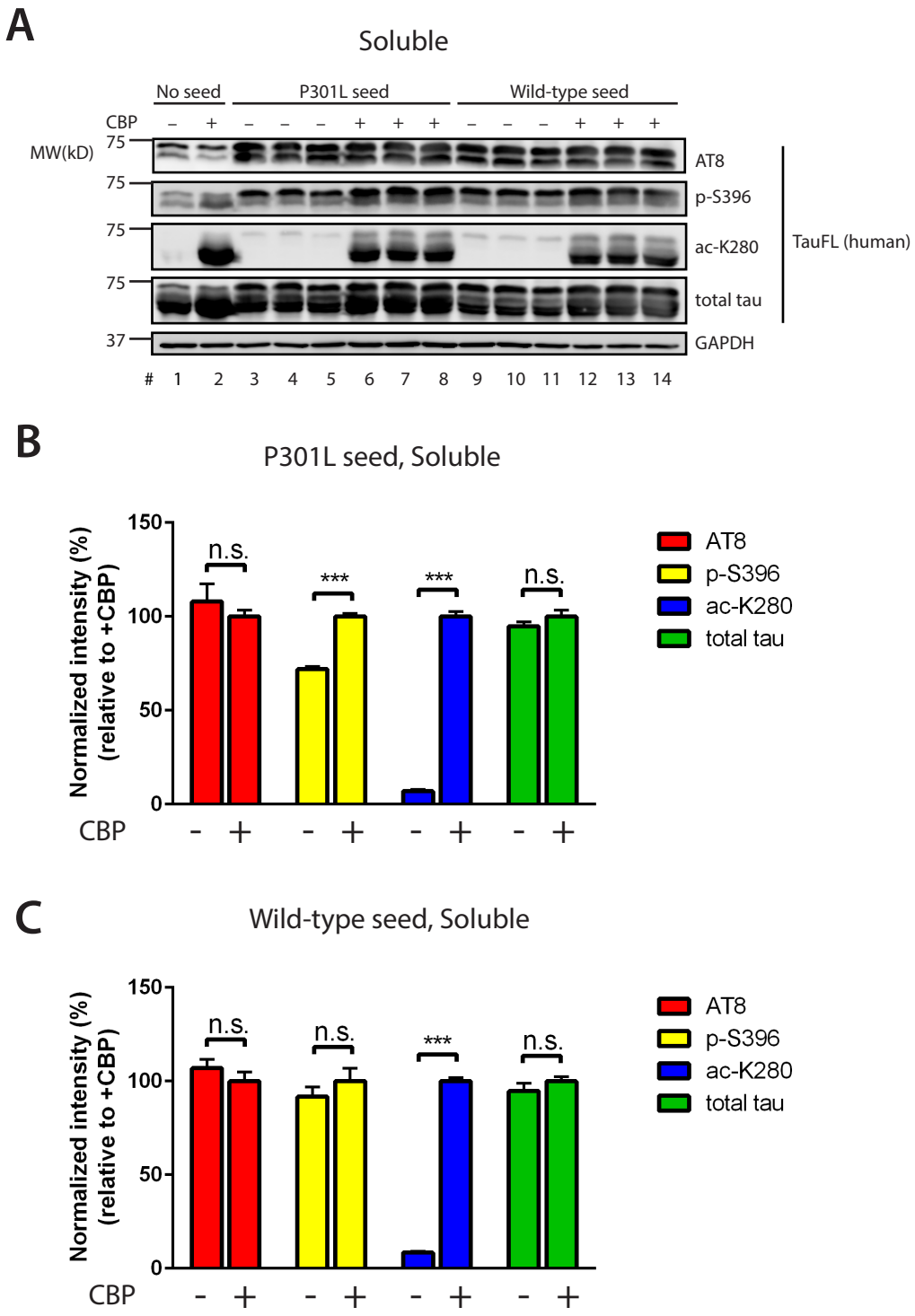

Figure S4. Cell-based tau seeding assay in the presence of ectopically expressed CBP acetyltransferase, Related to Figure 4

(A-C) 293A cells were transfected for 48 h with full-length P301L tau in the presence or absence of the acetyltransferase CBP. Wild-type or P301L tau seeds were then transduced into transfected cells to promote full-length tau templating and seeding. The cells were harvested and fractionated into soluble **(A)** and insoluble **(see Figure 4A)** fractions and the extent of full-length tau seeding was evaluated by immunoblotting with phosphorylated (AT8 and p-S396), acetylated (ac-K280) and total tau antibodies. Quantification of tau modification and seeding was determined by analysis of soluble **(B, P301L seed; C, wild-type seed)** or insoluble **(see Figure 4B-C)** fractions. Error bars indicate SEM; n = 3 biologically independent experiments. p value was determined by unpaired t test. n.s. $p > 0.05$, *** $p < 0.001$.

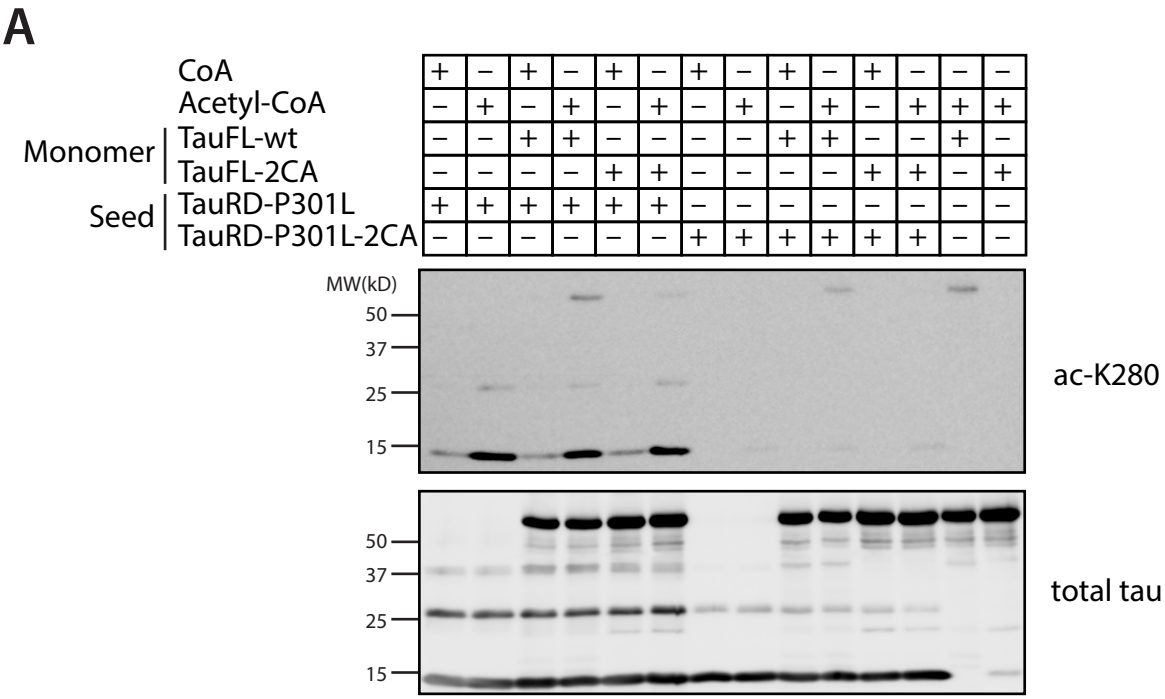

Figure S5. Wild-type full-length tau is unable to acetylate tau seeds *in vitro,* Related to Figure 5
(A) Recombinant P301L or P301L/C291A/C322A (P301L-2CA) tau seeds comprising the MTBR fragment were mixed with recombinant tauFL-wild-type or tauFL-2CA monomers in the presence of CoA or acetyl-CoA in acetylation reaction buffer for 1.5 h at 37 ˚C. The reaction was terminated by adding 6X gel loading buffer and analyzed by western blotting using acetylated (ac-K280) and total tau antibodies.

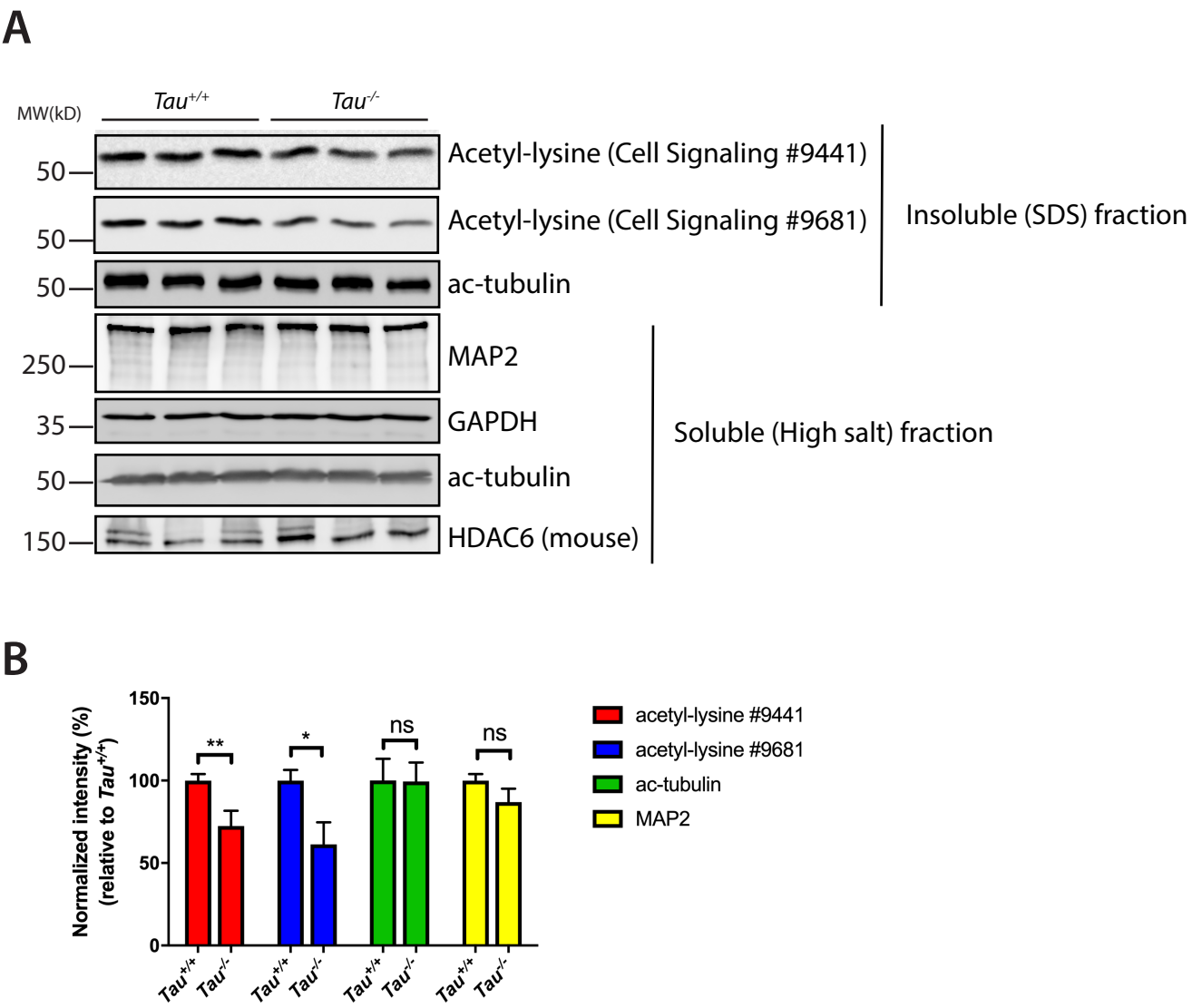

Figure S6. Tau depletion reduces acetyl-lysine immunoreactivity *in vivo*, Related to Figure 6

(A) Cortical brain tissue from *Tau*$^{+/+}$ or *Tau*$^{-/-}$ mice was harvested, homogenized, and fractionated into soluble (High Salt) and insoluble (SDS) fractions and analyzed by immunoblotting with two different pan-acetyl-lysine antibodies, as well as ac-tubulin and HDAC6 antibodies. MAP2 served as a marker for normal neuronal development and GAPDH served as a loading control.

(B) Quantification of the two pan-acetyl-lysine antibodies, ac-tubulin, and MAP2 between *Tau*$^{+/+}$ and *Tau*$^{-/-}$ mice. Error bars indicate SEM; n = 3 mice in each genotype. p value was determined by unpaired t test. n.s. $p > 0.05$, * $p < 0.05$, ** $p < 0.01$.

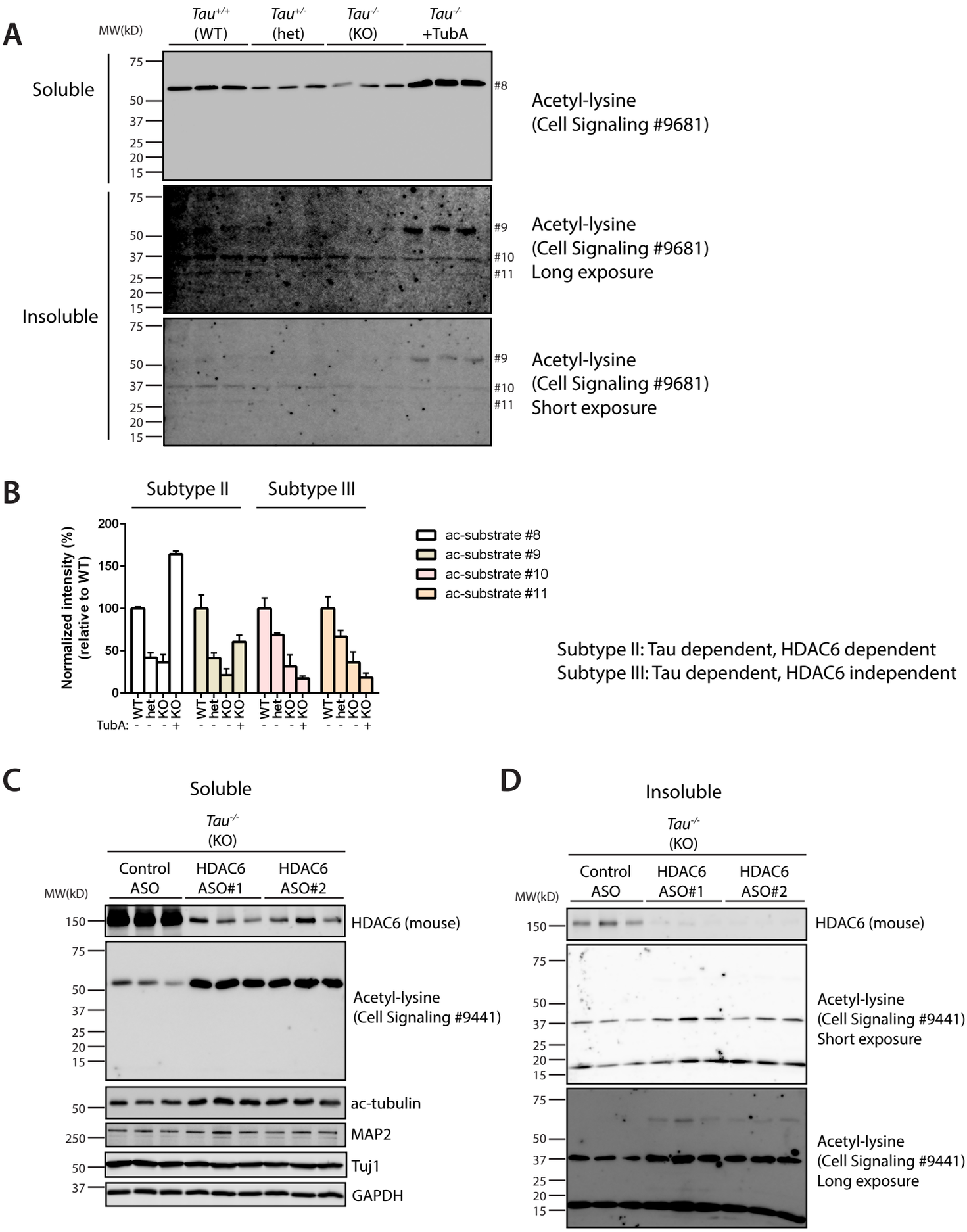

Figure S7. Tau depletion activates HDAC6 and leads to reduced acetyl-lysine immunoreactivity, Related to Figure 6

(A) Primary *Tau*$^{+/+}$, *Tau*$^{+/-}$, and *Tau*$^{-/-}$ neurons were left untreated or treated with TubA (1 μM) overnight, fractionated into soluble and insoluble fractions, and analyzed by immunoblotting with a pan-acetyl-lysine antibody to reveal changes in pan-acetylated substrates. Four distinct substrates were detected by acetyl-lysine immunoreactivity and numbered accordingly.

(B) The acetylation levels of four substrates were quantified and classified as subtypes I-III based on responsiveness to the HDAC6 inhibitor TubA (tau independent, HDAC6 dependent, subtype I), those that respond to both TubA and the presence of tau (tau dependent and HDAC6 dependent, subtype II), or those that respond only to the presence of tau alone (tau dependent, HDAC6 independent, subtype III).

(C-D) Primary *Tau*$^{-/-}$ neurons were treated with control or HDAC6 ASOs (10 μM), fractionated into soluble and insoluble fractions and analyzed by immunoblotting with HDAC6 and pan-acetyl-lysine antibodies to reveal lysine acetylation changes. Ac-tubulin served as a read-out for loss of HDAC6 activity. MAP2 and Tuj1 analysis revealed normal neuronal maturation and development in *Tau*$^{-/-}$ neurons. GAPDH served as loading control.

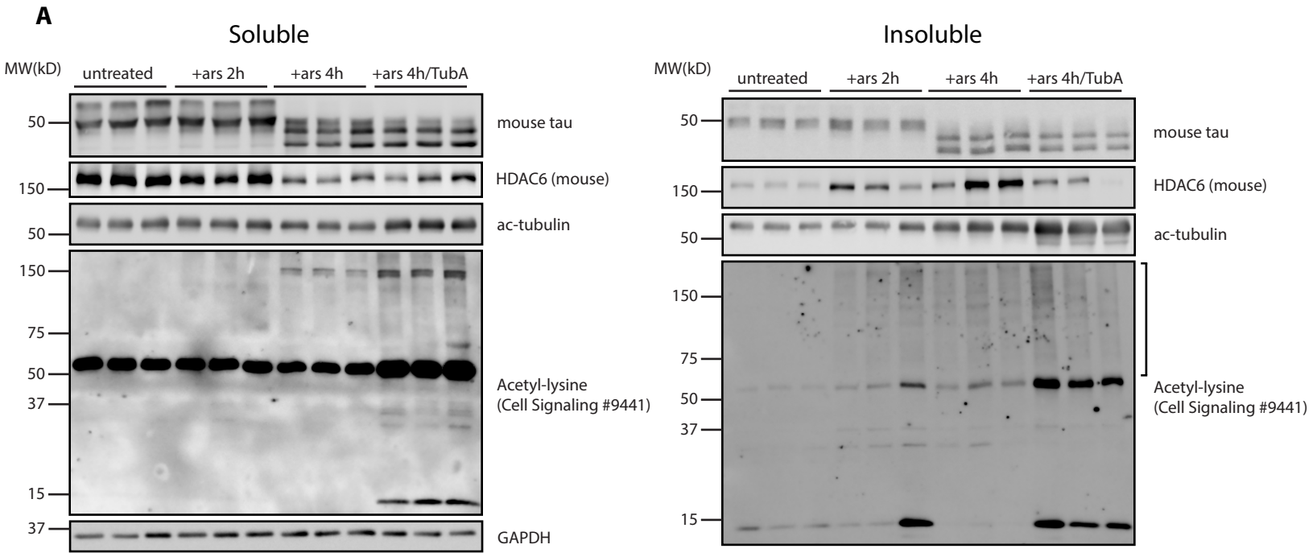

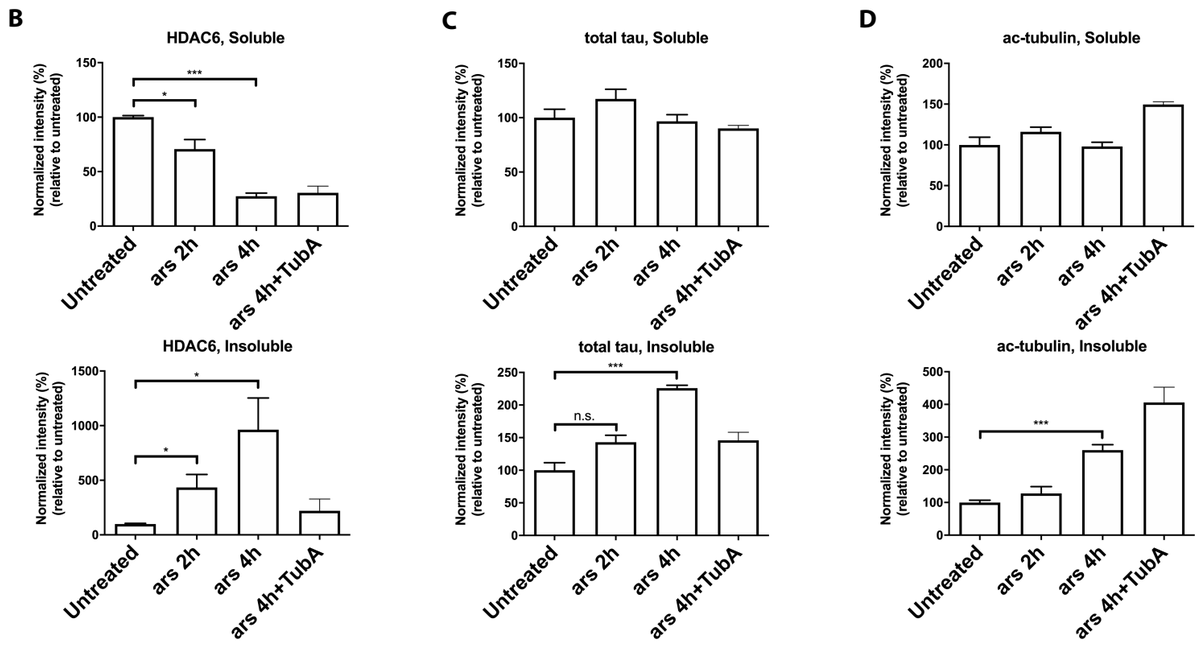

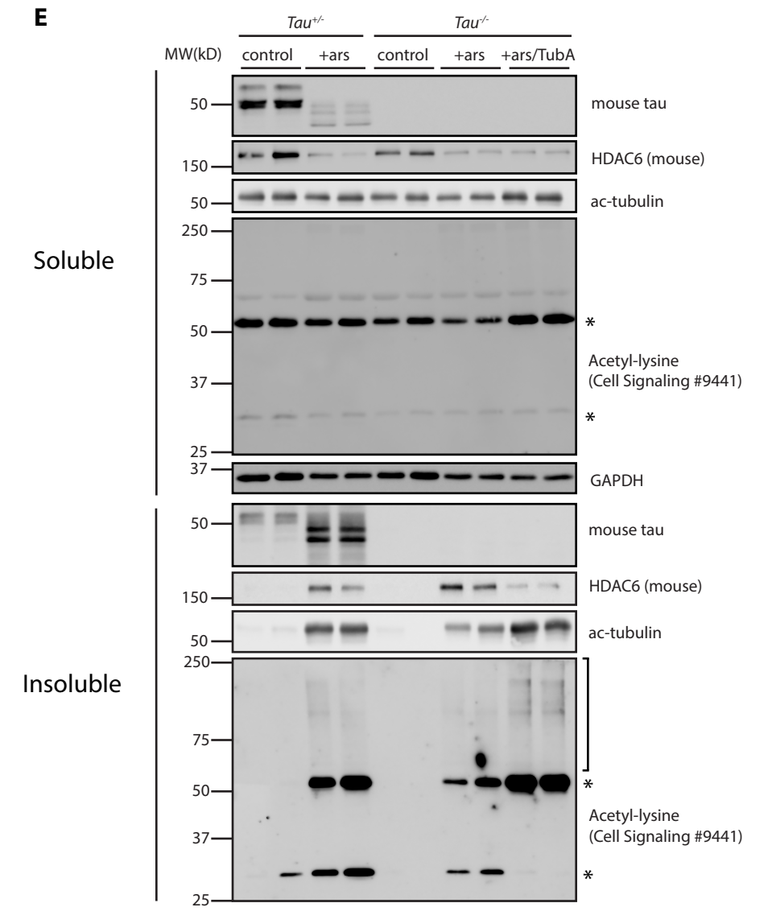

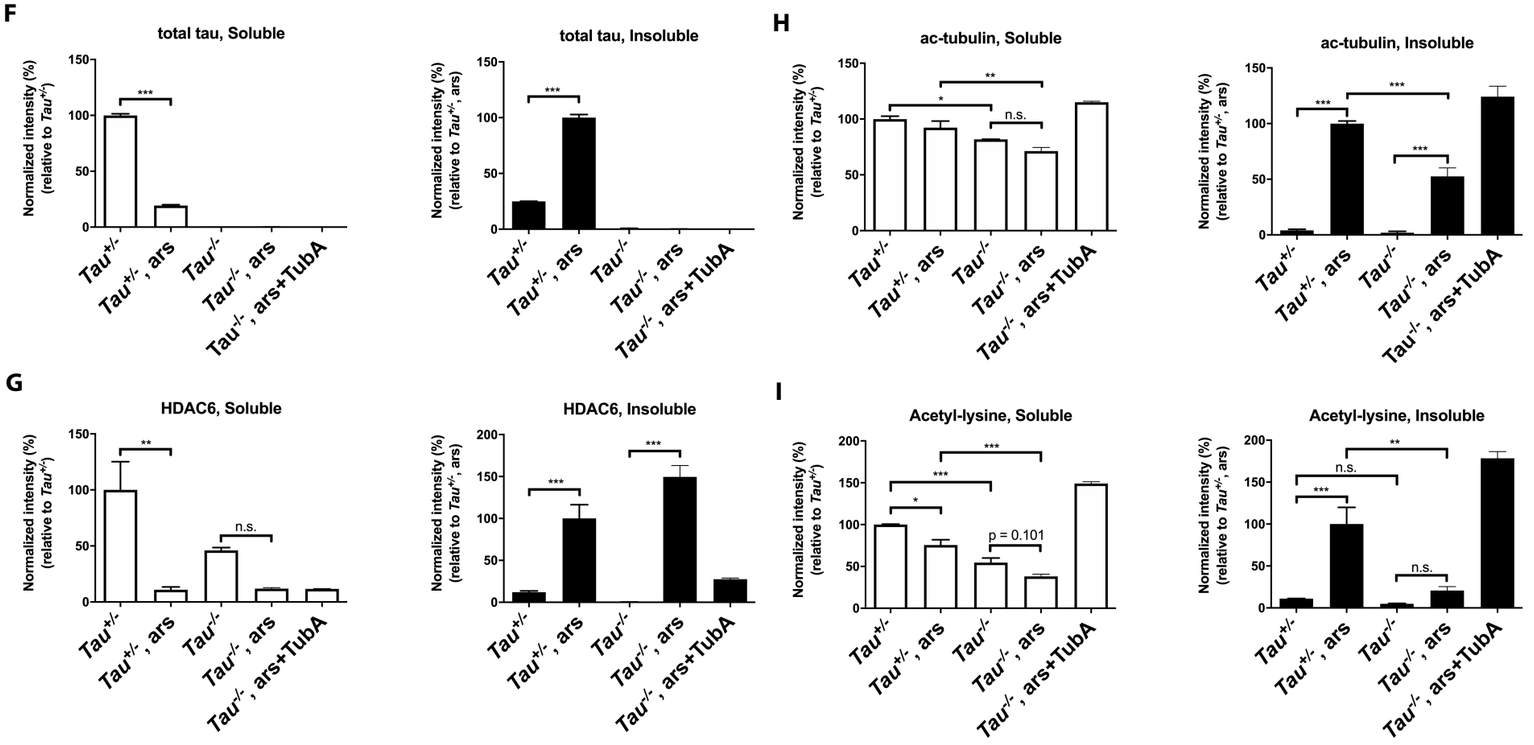

Figure S8. Oxidative stress causes insoluble HDAC6 accumulation and a corresponding increase in lysine acetylation that is suppressed by tau depletion, Related to Figure 7

(A) Primary wild-type neurons were untreated or treated with 0.25 mM sodium arsenite for 2 or 4 h in the absence or presence of TubA (5 μM). Cells were then harvested, fractionated into soluble and insoluble fractions, and analyzed by immunoblotting with total tau, total HDAC6, ac-tubulin, and pan-acetyl-lysine antibodies. GAPDH served as loading control. The insoluble protein bands highlighted by the bracket indicate acetylated high molecular weight aggregates.

(B-D) The levels of HDAC6 **(B)**, total tau **(C)**, and ac-tubulin **(D)** in either soluble or insoluble fraction were quantified and plotted relative to the control untreated sample. Error bars indicate SEM; n = 3 biologically independent experiments. p value was determined by unpaired t test. n.s. $p > 0.05$, * $p < 0.05$, *** $p < 0.001$.

(E) Primary *Tau*$^{+/-}$, and *Tau*$^{-/-}$ neurons were left untreated or treated with sodium arsenite (0.25 mM) for 4 h in the absence or presence of TubA (5 μM), fractionated into soluble and insoluble fractions, and analyzed by immunoblotting with total tau, total HDAC6, ac-tubulin, or pan-acetyl-lysine antibodies. The bracket represents insoluble, high molecular weight, acetylated protein aggregates. The asterisks (*) highlight the 50 kD and 30 kD acetylated substrates (#4 and #5).

(F-I) The levels of total tau **(F)**, total HDAC6 **(G)**, ac-tubulin **(H)**, or the 30 kD and 50 kD acetylated bands **(I)** in either soluble or insoluble fraction were quantified and plotted relative to the *Tau*$^{+/-}$ control. Error bars indicate SEM; n = 3 biologically independent experiments. p value in **(F)** was determined by unpaired t test. p value in **(G-I)** was determined by one-way ANOVA with Tukey's test for multiple comparisons among groups. * $p < 0.05$, ** $p < 0.01$, *** $p < 0.001$.

Positions in Protein	Sequence	Phosphorylation site	PhosphoRS localization (%)	Theo. MH+ [Da]	XCorr Score	Charge	m/z [Da]	DeltaM [ppm]
[18-32]	QNPQ**S**PPQDSSVTSK	S22	100	1679.72724	3.2	3	560.5811	0.82
[43-51]	**S**IPNLAEVK	S43	100	1050.5231	1.47	2	525.7654	0.36
[674-693]	YDHG**T**FFPMGDEGASSQIGR	T678	100	2251.91142	2.55	3	751.3072	-1.96

Table S1. HDAC6 phosphorylation sites detected by LC-MS/MS, Related to Figure 7

Mass spectrometry (MS) data are derived from the highest scoring phospho-peptide across the samples (n=2). For confident phosphorylation site localization within a peptide, a probability (0-100%) is calculated based on the detected product ions as determined by the phosphoRS algorithm.